Transition State Barriers in Multidimensional Marcus Theory

Jill Zwickl, Neil Shenvi, J. R. Schmidt, and John C. Tully*

Department of Chemistry, Yale University, New Haven, Connecticut 06520

Received: January 24, 2008; Revised Manuscript Received: August 4, 2008

Multidimensional Marcus theory is the extension of traditional Marcus theory to systems in which multiple particles are transferred. Rather than the intersecting parabolas of Marcus theory, multidimensional Marcus theory involves the intersection of paraboloids. In this paper, we examine the conditions under which a full multidimensional treatment of these paraboloids is necessary and when it is possible to use a simpler one-dimensional formalism. In particular, we examine transition state barrier energies, which are essential parameters in many reaction rate equations, and which depend on the formalism used. We find, based on both analytic calculations and numerical simulation, that the reduced one-dimensional treatment yields excellent agreement with the exact, multidimensional results over a wide variety of conditions for one particular choice of the single collective reaction coordinate. We also outline a procedure for calculating accurate multidimensional transition state barrier energies and apply it to a two-dimensional model of proton-coupled electron transfer.

I. Introduction

Electron and proton transfer are at the core of many important biological and chemical reactions. Especially in the case of biological reactions, the local environments of the charge donor and acceptor play a crucial role in determining the reaction rate. Over 50 years ago, Marcus realized the importance of the solvent environment in outer shell electron transfer, and developed a theory which has been central in understanding electron transfer ever since.[1−3]

Recently, there has been a growing interest in multiple charge transfer reactions,[4−6] of which proton-coupled electron transfer (PCET) is the most conspicuous example.[5,6] In such systems, more than one charged particle is transferred between solvated donor and acceptor molecules. This transfer can occur in a stepwise fashion, or as a single concerted reaction. The transferred species themselves may be identical (e.g., two electrons) or different (e.g., one electron and one proton). However, the starting point for the treatment of transfer reactions is almost always Marcus theory, appropriately modified for the treatment of multiple particles.

Marcus theory assumes that charge transfer occurs only when a solvent fluctuation temporarily destabilizes the reactant species or stabilizes the product species so that the donor and acceptor states are equienergetic. Charge transfer can be either adiabatic or nonadiabatic depending on the strength of coupling between the product and reactant electronic states. Because solvent dynamics govern the reaction, the reaction coordinate is assumed to be some collective function of the solvent variables which specifies the solvent stabilization of the donor and acceptor sites. Marcus showed that, within the assumptions of his model, the free energy of the reactant and product species as a function of the reaction coordinate could be described by two parabolas.[2] The intersection of these parabolas gives the transition state free energy barrier to the charge transfer reaction.

In the case of multiple charge transfer, there are several donor and acceptor sites, each of which can be solvated independently[7] (for instance, the proton and electron will each have their own separate solvation shell). Hence, multiple solvent coordinates are needed to specify the stabilization of each site. In this case, the one-dimensional (1D) Marcus theory free energy parabolas become multidimensional free energy paraboloids whose intersection again gives the reaction free energy barrier.[6] Because the intersection of two N-dimensional paraboloids is an $(N - 1)$-dimensional manifold, determining the exact transition state requires a minimization over this manifold to find the saddle point.

In this paper, we will examine the reaction free energy barrier in multidimensional Marcus theory. The barrier height, which is important for calculating rate constants, requires careful treatment when reducing the multidimensional problem to fewer dimensions. In particular, we will answer several questions. First, when does multiple charge transfer require multiple solvent coordinates? Can a single, collective solvent coordinate be used instead? Second, will the reaction path always lie directly on the line segment joining the two parabolic minima or can it lie elsewhere? Finally, how will nonlinear solvent response affect the location and height of the transition state free energy barrier? These topics will be addressed through careful theoretical development and numerical simulations. Although we will use PCET to illustrate and develop our theory, our conclusions can be applied to multidimensional Marcus theory in any multiple charge transfer system.

The paper is organized as follows. Section II provides background material on basic 1D Marcus theory, and introduces much of the notation to be used in later sections. The results in this section are relatively well-known, and a reader familiar with Marcus theory can easily skip this section. Section IIIA extends the 1D formalism to multiple dimensions. In sections IIIB and IIIC, we present our derivations for the linear and nonlinear solvent response regimes. Section IV gives the results of molecular dynamics (MD) simulations carried out on a model system, and compares the results of our theoretical analysis. Conclusions are presented in section V.

II. Background

A. 1D Marcus Theory. In its original formulation, Marcus theory was designed to predict the rate constant of outer-shell electron transfer between a donor and acceptor molecule in

* To whom correspondence should be addressed.

10.1021/jp805065g CCC: $40.75 © 2008 American Chemical Society
Published on Web 10/01/2008

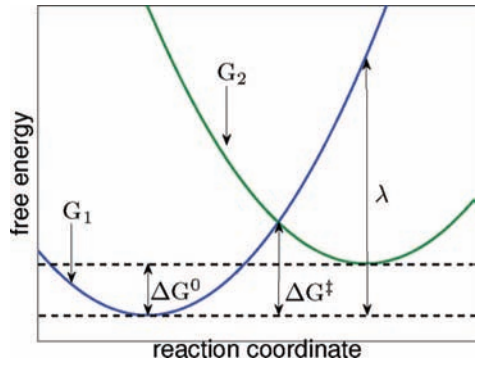

Figure 1. Marcus parabolas corresponding to the free energies of the reactant and product species. Electron transfer occurs at the intersection of the two curves, where the total energy of the reactant and product states are equal.

solution.[2] Marcus assumed a polarizable continuum solvent model, which led eventually to the famous Marcus equation for the transition state free energy barrier

$$\Delta G^{\ddagger} = \frac{(\Delta G^0 + \lambda)^2}{4\lambda} \tag{1}$$

where ΔG^0 is the difference in solvation free energies of product and reactant, and λ is the reorganization energy of the reactant (see Figure 1). Marcus theory requires that two major conditions are satisfied for Eq. (1) to be valid: first, electron transfer occurs only when the total energies of the solvated reactant and product are equal (i.e., that no light is emitted during electron transfer); second, the response of the solvent is linear with respect to the perturbations about the equilibrium state (i.e., the free energy is quadratic). The second condition was originally a consequence of Marcus' continuum solvent model, but is now often applied as an assumption even when there is an explicit molecular description of the solvent. In this latter case, some justification for this assumption can be found in the central limit theorem.[8,9] We will address the assumption of linear solvent response and its consequences for multidimensional Marcus theory in later sections.

The rate constant for an electron transfer reaction can be described by the transition state theory expression

$$k = \upsilon \exp(-\beta \Delta G^{\ddagger}) \tag{2}$$

where υ is a preexponential rate factor, $\beta = 1/k_B T$, and $\Delta G^{\ddagger}$ is the free energy barrier. Equation 2 is a simplified expression, because even in the limit of transition state theory, calculation of k involves Boltzmann weighted sums over any inner-shell vibronic states, and the calculation of Franck−Condon overlap factors of the associated vibrational wave functions.[10] In addition, the expression for the preexponential factor υ will depend on whether the reaction is nonadiabatic or adiabatic. If the coupling between the reactant and product states is large, then the transfer will proceed adiabatically. As the solvent undergoes fluctuations, the system will follow the electronic ground state, crossing over from the reactant to product parabola each time the transition state is traversed. In this case, the preexponential factor will be given by the inverse of the solvent fluctuation time scale. If the coupling between the reactant and product is small, then the transfer will be nonadiabatic. The system will tend to remain on the reactant parabola when the transition state is traversed, and the preexponential factor will be given by Fermi's golden rule evaluated at the transition state. In either case, the transition state free energy barrier $\Delta G^{\ddagger}$ appears explicitly in the rate constant expression. In this paper, we are not interested in calculating the rate contstant itself; rather we will focus on calculating $\Delta G^{\ddagger}$, which is an essential piece of the overall rate constant.

In standard Marcus theory, a single electron is transferred between a donor molecule D_e and an acceptor molecule A_e. The valence bond (VB) states corresponding to product and reactant for the electron transfer (ET) reaction $1 \rightarrow 2$ are

$$(1)\ D_e^{-1} - A_e$$
$$(2)\ D_e - A_e^{-1}$$

where D_e^{-1} and A_e^{-1} denote one electron on the donor and acceptor, respectively. The solute molecules interact with a collection of solvent molecules, whose configuration will be denoted by the variable ξ, which encompasses the coordinates of all of the solvent molecules. The energies of the VB states will therefore depend on the configuration of the surrounding solvent molecules in addition to the internal (gas phase) energy of the VB state itself. Thus, the total energy E_i of each VB state can be written as

$$E_i(\xi) = V(\xi) + \epsilon_i(\xi) + U_i \tag{3}$$

where $i = (1, 2)$. In eq 3, $V(\xi)$ is the energy of interaction between the solute molecules and the solvent (excluding the transferring electron), $\epsilon_i(\xi)$ is the interaction of the electron charge distribution with the solvent, and U_i is the internal (gas phase) energy of the VB state.

Marcus theory assumes that the transfer reaction can only occur when the total energies of state (1) and state (2) are equal for a given fixed solvation environment. From eq 3, the total energy is the sum of the solute−solvent interaction, the charge-solvent interaction and the internal energy. Since the solute−solvent interaction $V(\xi)$ is identical for states (1) and (2), the total energy difference is given by

$$\Delta E(\xi) = E_2(\xi) - E_1(\xi) \tag{4}$$
$$= \Delta\epsilon(\xi) + U_2 - U_1 \tag{5}$$

where

$$\Delta\epsilon(\xi) = \epsilon_2(\xi) - \epsilon_1(\xi) \tag{6}$$

The assumption that ET occurs when $\Delta E(\xi) = 0$ leads to the condition that at the transition state $\xi^{\ddagger}$, the solvation energy difference between the two VB states is equal to the negative internal energy difference

$$\Delta\epsilon(\xi^{\ddagger}) = -(U_2 - U_1) \tag{7}$$

We can then use the solvation energy difference, $\Delta\epsilon$, as the reaction coordinate,[11,12] defining the free energy of the reactant state as

$$G_1(x) = -\frac{1}{\beta} \ln \int \mathrm{d}\xi \delta(x - \Delta\epsilon(\xi)) \exp(-\beta E_1(\xi)) \tag{8}$$

The reaction barrier is given by the difference between the free energy at the transition state $x^{\ddagger}$ and at the reactant minimum x_1

$$\Delta G^{\ddagger} = G_1(x^{\ddagger}) - G_1(x_1) \tag{9}$$

One of the advantages of using $\Delta\epsilon$ as the reaction coordinate is that it provides an exact relation between the free energies of the product and reactant states.[12] To show this, we examine the free energy of the product state (2), which is given by

$$G_2(x) = -\frac{1}{\beta}\ln\int d\xi\delta(x-\Delta\epsilon(\xi))\exp(-\beta E_2(\xi)) \quad (10)$$

From eqs 3−6, eq 10 can be written as

$$G_2(x) = -\frac{1}{\beta}\ln\int d\xi\delta(x-\Delta\epsilon(\xi))\exp(-\beta(E_1(\xi)+\Delta\epsilon(\xi)+U_2-U_1)) \quad (11)$$

$$= -\frac{1}{\beta}\ln\int d\xi\delta(x-\Delta\epsilon(\xi))\exp(-\beta(E_1(\xi)+x+U_2-U_1)) \quad (12)$$

$$= x+U_2-U_1-\frac{1}{\beta}\ln\int d\xi\delta(x-\Delta\epsilon(\xi))\times\exp(-\beta E_1(\xi)) \quad (13)$$

$$G_2(x) = G_1(x)+x+U_2-U_1 \quad (14)$$

Equation 14, which was first derived by Warshel in ref 12, is an important result which has several consequences. First, it shows that the reactant and product free energy curves intersect at the transition state $x^\ddagger = -(U_2 - U_1)$. This fact is consistent with the energy conservation of the electron transfer event required by Marcus theory. Second, because eq 14 provides an exact relationship between the free energies $G_1(x)$ and $G_2(x)$, we can view $G_1(x)$ as the fundamental free energy surface, from which $G_2(x)$ is a derivative quantity.[13] If we further assume that the reactant free energy $G_1(x)$ is globally quadratic with respect to x, it follows that the product free energy $G_2(x)$ is a shifted parabola with the same curvature as $G_1(x)$. In fact, eq 14 provides justification for the often unspoken assumption that the reactant and product Marcus parabolas have the same curvature.

B. Calculation of the Free Energy Barrier. Having recounted the well-established formalism of 1D Marcus theory, we now turn our attention to numerical evaluation of the transition state barrier $\Delta G^\ddagger$. The free energy of the system can be obtained from molecular simulations by holding the solute fixed in the charge distribution corresponding to VB state (1) and averaging over many positions of the surrounding solvent molecules using Monte Carlo or MD techniques. During the simulation, the value of $\Delta\epsilon(\xi)$ is recorded and histogrammed. The free energy is then calculated by the standard equation

$$G_1(x) = -\frac{1}{\beta}\ln P(x) \quad (15)$$

where $P(x)$ is the estimated probability that $\Delta\epsilon(\xi) = x$.[12] In principle, the free energy barrier $\Delta G^\ddagger$ can be calculated directly from such a simulation. In practice, the values of $\Delta\epsilon(\xi)$ cluster around the free energy minimum at x_1, and will rarely probe the transition state region at $x^\ddagger = -(U_2 - U_1)$.

It is here that the assumption of linear solvent response is normally invoked. If the solvent responds linearly to a perturbation in x from its equilibrium value, the free energy function will be a quadratic function of x. Within this approximation, the position and curvature of the free energy minimum can be used to extrapolate the free energy to its value in regions far from equilibrium. Evaluating the extrapolated free energy at the transition state then yields the free energy barrier $\Delta G^\ddagger$ (see Figure 2a).

The procedure described above requires as input the data from a single computer simulation of the solvent fluctuations about the reactant state (1). Alternatively, separate data could be obtained for simulations of both state (1) and state (2). Assuming the solvent response is globally linear, the resulting parabolas will be shifted in energy and position, but have the same curvature (see eq 14 and Figure 2a). The intersection of these parabolas is the transition state, and the energy difference between the transition state and the reactant free energy minimum yields the free energy barrier, in agreement with eq 1.

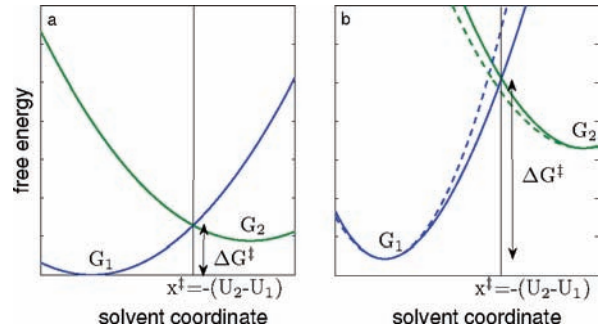

Figure 2. Illustration of the difficulties of approximating the free energy barrier using a quadratic expansion of the reactant and product free energies about their minima. Panel a shows the case where the solvent response is linear. In this case, the parabolas have identical curvatures and intersect at $x^\ddagger = -(U_2 - U_1)$. Quadratic extrapolation then yields the correct free energy barrier. Panel b shows the case where solvent response is not globally linear. The solid lines show the true, nonquadratic free energy curves, which satisfy eq 14 and intersect at $x^\ddagger = -(U_2 - U_1)$. The dashed lines show the quadratic fit to these curves about their minima. The quadratic fit yields curves which do not intersect at $x^\ddagger = -(U_2 - U_1)$ and does not provide a correct free energy barrier.

However, in practice numerical simulations demonstrate that the two parabolas often have different curvatures, resulting in seeming inconsistencies with eqs 7 and 14 (see Figure 2b). What is going on? The answer is that although eq 14 is exact, the assumption that $G_1(x)$ is globally quadratic is false. $G_1(x)$ (or $G_2(x)$) may appear quadratic about its minimum in the region sampled by the computer simulation, but at distant values of x, it may deviate from quadratic behavior. For example, it has been shown that, when the different electronic states of the electron donor−acceptor complex have different polarizabilities, the resulting global free energy can be distinctly nonquadratic.[14,15] It is again helpful to think of $G_1(x)$ as the only physical free energy surface, which can be sampled by placing the solute in the VB state (1) and simulating solvent fluctuations. Simulations of the VB state (2) can be thought of as sampling the surface $G_1(x)$ with an additional biasing potential $+x$, so that a different region of the variable x is sampled. The "correct" answer is then obtained by combining the data from these two simulations to obtain a nonquadratic (i.e., quartic or higher-order multinomial) fit to $G_1(x)$, as in ref 16. In section IIIC, we will examine how nonlinear solvent response affects the calculation of free energy barriers in multidimensional Marcus theory and will suggest a method by which accurate representations of nonquadratic free energy surfaces can be constructed.

III. Theory

A. Multidimensional Marcus Theory. Having discussed basic 1D Marcus theory at length, we now turn our attention to multidimensional Marcus theory, in which multiple charged particles are transferred between a donor and acceptor molecule. In what follows, we will consider systems in which two particles are transferred; the results are easily generalized to more than two particles. We have chosen to develop our theory within the framework of proton-coupled electron transfer; however, our theory would be equally applicable to any application of

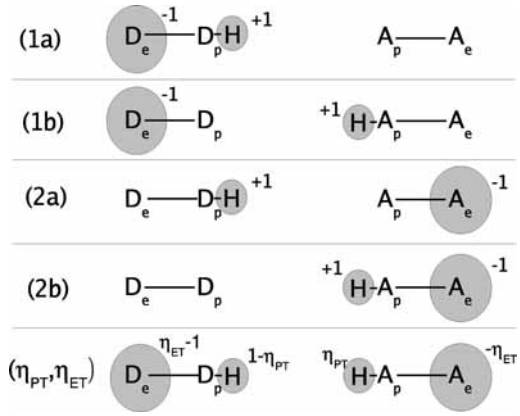

Figure 3. Four VB states (1a, 1b, 2a, and 2b) and the fictitious partial charge transfer state (η_{PT} and η_{ET}). During PCET, an electron is transferred from the electron donor D_e to electron acceptor A_e and the proton is transferred from the proton donor D_p to the proton acceptor A_p.

multidimensional Marcus theory, such as two-electron transfer. As mentioned in section II, our goal is to determine when, and how, the multidimensional case may be reduced to fewer dimensions. In order to do this, we will focus on calculating free energy barriers, since these parameters depend on the formalism used and are essential for calculating rate constants. However, our intent is not to calculate the rate constants themselves, so we will not include calculations for the numerous factors which enter into the rate equations.

Following the notation of Soudackov et al.,[5,17] let us consider the four valence bond (VB) states in Figure 3, in which D_e and D_p are the electron and proton donors and A_e and A_p are the electron and proton acceptors, respectively. Thus, the reactions 1a → 2b and 2a → 2b involve proton transfer (PT), the reactions 1a → 2b and 1a → 2b involve electron transfer (ET), and the reaction 1a → 2b involves proton-coupled electron transfer (PCET). In this paper, we are specifically interested in the concerted PCET reaction 1a → 2b, in which the proton and electron are transferred simultaneously rather than in a stepwise fashion. Such a mechanism will be favored if, for instance, the internal energies of states 1b and 2a are high due to charge separation.

Rate constants for concerted PCET reactions have been derived by Soudackov and Hammes-Schiffer[7] and in the high-temperature limit involve a free energy barrier

$$\Delta G^{\ddagger}_{2D} = \frac{(\Delta G^{0}_{2D} + \lambda_{2D})^2}{4\lambda_{2D}} \tag{16}$$

The resulting PCET rate expression involves Boltzmann weighted sums over proton vibronic states, and the calculation of Franck−Condon overlap factors of the proton vibrational wave functions.[17,18] However, once again we focus our attention only on the free energy barrier.

As before, reactant and product molecules interact with a collection of solvent molecules so that the total energy E_i of each VB state can be written as

$$E_i(\xi) = V(\xi) + \epsilon_i(\xi) + U_i \tag{17}$$

where the terms are defined in section II, and i = 1a, 1b, 2a, and 2b. Based on these definitions, we can define the variables

$$\Delta\epsilon_{PT}(\xi) = \epsilon_{1b}(\xi) - \epsilon_{1a}(\xi) \tag{18}$$

$$\Delta\epsilon_{ET}(\xi) = \epsilon_{2a}(\xi) - \epsilon_{1a}(\xi) \tag{19}$$

$$\Delta\epsilon_{PCET}(\xi) = \epsilon_{2b}(\xi) - \epsilon_{1a}(\xi) \tag{20}$$

corresponding to the energies of PT, ET, and PCET, respectively.

If we make the common assumption[12,19−21,17] that the interaction of the solvent with electron/proton is linear with respect the solute charge distribution, then

$$\Delta\epsilon_{PCET}(\xi) = \Delta\epsilon_{PT}(\xi) + \Delta\epsilon_{ET}(\xi) \tag{21}$$

reducing the number of reaction coordinates from three (see eqs 18−20) to two. This assumption is valid if the solvent molecules are not internally polarizable, as is the case in our MD simulations. Note that we are assuming that the solute−solvent interaction energy $\epsilon_i(\xi)$ is a linear functional of the charge distribution, but we are not assuming that the system free energy $G_i(x)$ responds linearly to charge. We will examine the effects of solvent nonlinearity on reaction free energy barriers in section IV.

The relationship between $G_1(x)$ and $G_2(x)$ in 1D Marcus theory can be extended to the multidimensional case. We define the free energy of each VB state as a function of the PT and ET energy differences

$$G_{1a}(x,y) = -\frac{1}{\beta}\ln\int \mathrm{d}\xi\,\delta(x - \Delta\epsilon_{PT}(\xi))\delta(y - \Delta\epsilon_{ET}(\xi)) \times \exp(-\beta E_{1a}(\xi)) \tag{22}$$

Then in analogy to eq 14, the free energy surfaces for the other three VB states are given by

$$G_{1b}(x,y) = G_{1a}(x,y) + x + U_{1b} - U_{1a} \tag{23}$$

$$G_{2a}(x,y) = G_{1a}(x,y) + y + U_{2a} - U_{1a} \tag{24}$$

$$G_{2b}(x,y) = G_{1a}(x,y) + x + y + U_{2b} - U_{1a} \tag{25}$$

Although the calculation of the free energy surface is similar in the 1D and 2D cases, the determination of the transition state presents some subtleties in multiple dimensions. The free energy surface $G_{1a}(x,y)$ can be obtained through molecular simulation of the solvent fluctuations about the reactant (1a) VB state, as in the 1D case. A histogram of the values of the ET and PT variables $\Delta\epsilon_{ET}(\xi)$ and $\Delta\epsilon_{PT}(\xi)$ then yields $G_{1a}(x,y)$. However, in the two-dimensional (2D) case, the transition state satisfies the equation

$$x^{\ddagger} + y^{\ddagger} = -(U_{2b} - U_{1a}) \tag{26}$$

Hence, there is an infinite line of points along which $G_{1a}(x,y)$ and $G_{2b}(x,y)$ intersect. To find the unique transition state $(x^{\ddagger},y^{\ddagger})$, $G_{1a}(x,y)$ must be minimized over the line which satisfies eq 26. As in one dimension, the free energy barrier is given by the difference between the free energy at the transition state and at the reactant free energy minimum

$$\Delta G^{\ddagger} = G_{1a}(x^{\ddagger}, y^{\ddagger}) - G_{1a}(x_{1a}, y_{1a}) \tag{27}$$

Figure 4 shows a schematic diagram of the two free energy surfaces G_{1a} and G_{2b} along with their line of intersection satisfying eq 26 (the dash-dotted line in Figure 4).

In the next section we derive expressions for the 2D transition state and corresponding activation energy for a concerted PCET reaction, assuming a linear solvent response. We show that, in the case of linear solvent response, the transition state in these reactions lies on the line segment joining the minima of the two free energy surfaces, x_{1a} and x_{2b} (see the solid line in Figure 4), and thus the results can be analyzed using traditional Marcus theory along the 1D slice through the 2D free energy surface. Of course, generating such a slice intrinsically requires the full

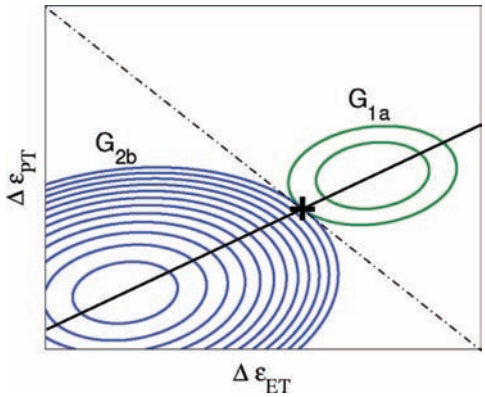

Figure 4. Schematic illustration of the 2D free energy surfaces. The transition state lies somewhere along the dash-dotted line which satisfies eq 26. The problem of finding the exact transition state can be approximated by reducing the free energy as a one-dimensional function by either (1) taking a cross section of the 2D free energy along the line connecting the two minima (the solid line) or (2) integrating the 2D free energy over the coordinate perpendicular to the PCET coordinate to obtain a 1D free energy as a function of the PCET coordinate, $\Delta\epsilon_{PCET} = \Delta\epsilon_{PT} + \Delta\epsilon_{ET}$. In section IIIB, we show that both of these methods yield the exact 2D free energy barrier (the + mark) in the limit, shown here, of quadratic free energy.

2D free energy surface, and obtaining such a 2D free energy surface can be costly.

In order to reduce the free energy surface to an effective 1D problem, we could sample alternatively G_{1a} and G_{2b} as functions of only the PCET variable $\Delta\epsilon_{PCET}$, rather than as functions of $\Delta\epsilon_{ET}$ and $\Delta\epsilon_{PT}$; this method would be equivalent to projecting the 2D free energy surfaces $G_{1a}(x,y)$ and $G_{2b}(x,y)$ onto the PCET coordinate $x + y$ and integrating out the remaining dimension. Once the problem is reduced to a single dimension, Marcus theory could be applied to calculate the resulting (reduced) free energy of activation. Although this technique has been used in the literature,[22,23] the relationship between the 2D and reduced 1D activation energies has not been established. In the next section, we will provide theoretical justification for this method in the limit of linear solvent response.

B. Calculation of Energy Free Barrier: Linear Solvent Response. The assumption of linear solvent response is ubiquitous in studies of electron and proton transfer. Originally, this linearity was derived as a consequence of the dielectric continuum solvent model used by Marcus; however, it has been found to be a useful assumption even when a molecular model of solvent is used. It must be stated at the outset that the solvent response will always be linear for small perturbations about the free energy minimum, resulting in a locally quadratic free energy. However, we here refer to an assumption of globally linear solvent response, resulting in a free energy which is quadratic everywhere. Such an assumption may be invalid at large displacements from equilibrium, such as at the transition state, but it allows for substantial simplification in sampling the free energy.

In a general PCET reaction, the donor and acceptor molecules will be chemically distinct species such that the internal energies are not equal ($U_{1a} \neq U_{2b}$). The free energies of the reactant and product states are related by eq 25. To simplify notation, let

$$\mathbf{x} = \begin{pmatrix} x \\ y \end{pmatrix}, \quad \mathbf{1} = \begin{pmatrix} 1 \\ 1 \end{pmatrix}, \quad \boldsymbol{\eta} = \begin{pmatrix} \eta_{PT} \\ \eta_{ET} \end{pmatrix} \tag{28}$$

If the solvent response is globally linear, we obtain the quadratic free energy surfaces

$$G_{1a}(\mathbf{x}) = \mathbf{x}^T A\mathbf{x} + \mathbf{b}^T\mathbf{x} + U_{1a} \tag{29}$$

$$G_{2b}(\mathbf{x}) = \mathbf{x}^T A\mathbf{x} + (\mathbf{b} + \mathbf{1})^T\mathbf{x} + U_{2b} \tag{30}$$

where A is the Hessian matrix of the free energy paraboloids

$$A = \begin{pmatrix} A_{xx} & A_{xy} \\ A_{xy} & A_{yy} \end{pmatrix} \tag{31}$$

and $\mathbf{b}$ is the linear term which determines the location of the free energy minimum. Equation 30 follows directly from eq 25. Equations 29 and 30 can be rewritten in the more standard form

$$G_{1a}(\mathbf{x}) = (\mathbf{x} - \mathbf{x}_{1a})^T A(\mathbf{x} - \mathbf{x}_{1a}) + U_{1a} - \mathbf{x}_{1a}{}^T A\mathbf{x}_{1a} \tag{32}$$

$$G_{2b}(\mathbf{x}) = (\mathbf{x} - \mathbf{x}_{2b})^T A(\mathbf{x} - \mathbf{x}_{2b}) + U_{2b} - \mathbf{x}_{2b}{}^T A\mathbf{x}_{2b} \tag{33}$$

where

$$\mathbf{x}_{1a} = -\frac{1}{2}A^{-1}\mathbf{b} \tag{34}$$

$$\mathbf{x}_{2b} = -\frac{1}{2}A^{-1}(\mathbf{b} + \mathbf{1}) \tag{35}$$

1. Exact 2D Treatment. As shown above, the free energy surfaces will intersect at the line specified by eq 26. To determine the exact location of the transition state, and hence the barrier height, we must minimize the free energy $G_{1a}(x,y)$ subject to the constraint in eq 26. Applying the method of Lagrange multipliers, we find that the transition state must satisfy the equation

$$\mathbf{x}^{\ddagger} = -\frac{1}{2}tA^{-1}\mathbf{1} + \mathbf{x}_{1a} \tag{36}$$

where t is an undetermined coefficient. Solving for eqs 26 and 36, we obtain the transition state

$$\mathbf{x}^{\ddagger} = -\left(\frac{U_{2b} - U_{1a} + \mathbf{1}^T\mathbf{x}_{1a}}{\mathbf{1}^T A^{-1}\mathbf{1}}\right)A^{-1}\mathbf{1} + \mathbf{x}_{1a} \tag{37}$$

$$= 2\left(\frac{U_{2b} - U_{1a} + \mathbf{1}^T\mathbf{x}_{1a}}{\mathbf{1}^T A^{-1}\mathbf{1}}\right)(\mathbf{x}_{2b} - \mathbf{x}_{1a}) + \mathbf{x}_{1a} \tag{38}$$

where eq 38 follows from eqs 34 and 35. It is clear from eq 38 that the transition state lies on the line joining the two minima $\mathbf{x}_{1a}$ and $\mathbf{x}_{2b}$. To arrive at this result, we have only assumed a globally linear solvent response, with no other constraints on the shape of the paraboloid or the position of the minima.

Finally, we can substitute eq 38 into eqs 27 and 32 to obtain the exact multidimensional free energy barrier

$$\Delta G^{\ddagger}_{2D} = \frac{(U_{2b} - U_{1a} + \mathbf{1}^T\mathbf{x}_{1a})^2}{\mathbf{1}^T A^{-1}\mathbf{1}} \tag{39}$$

Defining

$$\lambda_{2D} = G_{1a}(\mathbf{x}_{2b}) - G_{1a}(\mathbf{x}_{1a}) \tag{40}$$

$$\Delta G^{0}_{2D} = G_{2b}(\mathbf{x}_{2b}) - G_{1a}(\mathbf{x}_{1a}) \tag{41}$$

we find

$$\lambda_{2D} = \frac{1}{4}\mathbf{1}^T A^{-1}\mathbf{1} \tag{42}$$

$$\Delta G^{0}_{2D} = U_{2b} - U_{1a} + \mathbf{1}^T\mathbf{x}_{1a} - \frac{1}{4}\mathbf{1}^T A^{-1}\mathbf{1} \tag{43}$$

and thus

$$\Delta G^{\ddagger}_{2D} = \frac{(\Delta G^0_{2D} + \lambda_{2D})^2}{4\lambda_{2D}} \tag{44}$$

as expected.

Since both the reactant and product minima, as well as the transition state, lie on the line segment connecting the reactant and product minima, we can focus on a slice through the 2D free energy surface along this line. Therefore, in the limit of globally linear solvent response, taking a cross section of the free energy surface along the line between the two minima (i.e., the solid line in Figure 4), and applying standard Marcus theory will yield the correct transition state barrier. It is readily apparent that the free energy difference and reorganization energies of the Marcus parabolas resulting from this slice through the 2D free energy surface are ΔG^0_{2D} and λ_{2D}, respectively. Although such a treatment does intrinsically require the costly calculation of the full 2D surface, the analysis of the data is facilitated by creating such a 1D slice.

2. Reduced 1D Treatment. In order to avoid the costly 2D surface calculation, we next examine the technique of projecting the 2D free energy (via the associated probability distribution) onto a single coordinate $\Delta\epsilon_\theta$, where θ is the angle along which the free energy is projected. We will show that if the free energy is projected onto the PCET variable $\Delta\epsilon_{PCET} = \Delta\epsilon_{ET} + \Delta\epsilon_{PT}$ (i.e., $\theta = \pi/4$), then the effective 1D free energy barrier obtained is identical to the exact multidimensional result.

In general, an $(N-1)$-dimensional reduced free energy can be obtained from an N -dimensional free energy function by integrating the N -dimensional probability distribution over one of the independent coordinates. For instance, we can obtain the 1D reduced free energy $G_{1a}(x)$ from the 2D free energy $G_{1a}(x,y)$ from

$$G_{1a}(x) = -\frac{1}{\beta}\ln\left(\int \mathrm{d}y \exp(-\beta G_{1a}(x,y))\right) \tag{45}$$

$$= -\frac{1}{\beta}\ln\left(\int \mathrm{d}y\, P(x,y)\right) \tag{46}$$

Thus, to obtain the reduced 1D free energy $G_{1a}(x')$, which depends on the rotated coordinate x', from the 2D free energy $G_{1a}(x)$, we first write down the probability distribution $P(x)$, which is a Gaussian distribution since the free energy $G_{1a}(x)$ is quadratic in x (see eq 32)

$$P(x) = N\exp(-\beta G_{1a}(\mathbf{x})) \tag{47}$$

$$= N\exp\left(-\beta\left((\mathbf{x}-\mathbf{x}_{1a})^{\mathrm{T}}A(\mathbf{x}-\mathbf{x}_{1a}) + U_{1a} - \mathbf{x}_{1a}{}^{\mathrm{T}}A\mathbf{x}_{1a}\right)\right) \tag{48}$$

where N is an appropriate normalization constant. Next, we make a coordinate transformation using the rotation matrix R where

$$R = \begin{pmatrix} \cos\theta & \sin\theta \\ -\sin\theta & \cos\theta \end{pmatrix} \tag{49}$$

so that

$$\mathbf{x}' = \begin{pmatrix} x' \\ y' \end{pmatrix} = R\begin{pmatrix} x \\ y \end{pmatrix} \tag{50}$$

$$\mathbf{x}'_{1a} = R\mathbf{x}_{1a} \tag{51}$$

$$\mathbf{x}'_{2b} = R\mathbf{x}_{2b} \tag{52}$$

$$A' = RAR^{\mathrm{T}} \tag{53}$$

Transforming to the new coordinate system and integrating over y', we obtain the effective reduced probability distribution

$$P(x') = N\int \mathrm{d}y' \exp[-\beta((\mathbf{x}'-\mathbf{x}'_{1a})^{\mathrm{T}}A'(\mathbf{x}'-\mathbf{x}'_{1a}) + U_{1a} - \mathbf{x}'_{1a}{}^{\mathrm{T}}A'\mathbf{x}'_{1a})] \tag{54}$$

$$= N\sqrt{\frac{\pi}{\beta A'_{yy}}}\exp\left[-\beta\left(\left(A'_{xx} - \frac{A'^{\,2}_{xy}}{A'_{yy}}\right)(x'-x'_{1a})^2 + U_{1a} - \mathbf{x}'_{1a}{}^{\mathrm{T}}A'\mathbf{x}'_{1a}\right)\right] \tag{55}$$

Up to an overall constant, the corresponding 1D free energy is then

$$G_{1a}(x') = \left(A'_{xx} - \frac{A'^{\,2}_{xy}}{A'_{yy}}\right)(x'-x'_{1a})^2 + U_{1a} - \mathbf{x}'_{1a}{}^{\mathrm{T}}A'\mathbf{x}'_{1a} \tag{56}$$

Similarly, the 1D free energy for state (2b) is given by

$$G_{2b}(x') = \left(A'_{xx} - \frac{A'^{\,2}_{xy}}{A'_{yy}}\right)(x'-x'_{2b})^2 + U_{2b} - \mathbf{x}'_{2b}{}^{\mathrm{T}}A'\mathbf{x}'_{2b} \tag{57}$$

From eqs 56 and 57, it is clear that the two projected parabolas have identical curvatures. Then we can use the Marcus equation for the activation energy at their intersection

$$\Delta G^{\ddagger}_{1D} = \frac{(\Delta G^0_{1D} + \lambda_{1D})^2}{4\lambda_{1D}} \tag{58}$$

where

$$\lambda_{1D} = G_{1a}(x'_{2b}) - G_{1a}(x'_{1a}) \tag{59}$$

$$\Delta G^0_{1D} = G_{2b}(x'_{2b}) - G_{1a}(x'_{1a}) \tag{60}$$

Using eqs 56 and 57 to evaluate eqs 59 and 60, we obtain

$$\lambda_{1D} = \left(A'_{xx} - \frac{A'^{\,2}_{xy}}{A'_{yy}}\right)(x'_{2b} - x'_{1a})^2 \tag{61}$$

$$\Delta G^0_{1D} = \Delta G^0_{2D} \tag{62}$$

Equation 61 provides the reorganization energy between the reactant and product when projected onto an arbitrary reaction coordinate θ. However, if we choose $\theta = \pi/4$, which corresponds to the PCET variable $\Delta\epsilon_{PCET} = \Delta\epsilon_{ET} + \Delta\epsilon_{PT}$ and use the relationship between $\mathbf{x}_{1a}$ and $\mathbf{x}_{2b}$ (see eqs 34 and 35), we obtain

$$\lambda_{PCET} = \frac{\mathbf{1}^{\mathrm{T}}A^{-1}\mathbf{1}}{4} \tag{63}$$

We can then substitute eqs 63 and 64 into eq 65 to obtain the 1D activation energy

$$\Delta G^{\ddagger}_{PCET} = \frac{(U_{2b} - U_{1a} + \mathbf{1}^{\mathrm{T}}\mathbf{x}_{1a})^2}{\mathbf{1}^{\mathrm{T}}A^{-1}\mathbf{1}} \tag{64}$$

Equation 64 shows that the activation energy obtained by projection along $\theta = \pi/4$ is identical to the exact 2D activation energy in eq 39. Thus the exact, 2D activation energy is identical to the 1D free energy as a function of the PCET variable $\Delta\epsilon_{PCET}$ when the solvent response is linear. During an MD simulation, only the values of $\Delta\epsilon_{PCET}$ need to be recorded and histogrammed to yield the 1D free energy $G_{1a}(x')$, which will then yield the

exact multidimensional activation energy at the transition state $x'^{\ddagger} = -(U_{2b} - U_{1a})$.

As an aside, it is also interesting to analyze the results of the previous subsection in the context of standard adiabatic transition state theory (TST). In such cases a multidimensional free energy landscape is partitioned into reactant and product subspaces by an appropriately chosen dividing surface, and the transition state rate constant (or equivalently, free energy barrier) is determined by the flux passing through the dividing surface.[24] The choice of this dividing surface is arbitrary, but since TST provides an upper bound on the rate constant, the variationally "best" choice can be defined as the one yielding the lowest rate (or equivalently, highest free energy barrier). Connecting with the above results, the choice of reaction coordinate, via θ, also implicitly defines a dividing plane orthogonal to this reaction coordinate. It is not hard to show that the PCET reaction coordinate ($\theta = \pi/4$) corresponds to the highest free energy barrier, and thus the variationally optimal TST choice.

In conclusion, the derivations in the preceding section demonstrate that calculation of the multidimensional free energy barrier can be simplified to a 1D problem provided that the solvent response is linear. The exact transition state found through minimizing the free energy over the intersection of the two multidimensional paraboloids lies directly on the line segment joining the reactant (1a) and product (2b) free energy minima. In addition, writing the free energy as a function of only the PCET coordinate $\Delta\epsilon_{PCET}$ will also give the exact multidimensional free energy barrier. However, in many systems, the nonlinearity of the solvent response might be expected to render these approximations inaccurate; we examine the magnitude of these effects in the next section for a particular model system of PCET.

C. Nonlinear Solvent Response. In the previous subsection, we derived the activation energies for PCET within the assumption that the solvent response was linear (i.e., that the free energy surfaces were quadratic). In such cases, to obtain the activation energy from MD simulation, a 1D simulation of solvent fluctuations around only a single valence bond state need be performed and the results extrapolated assuming a paraboloid form for the free energy. From this single simulation, the exact multidimensional free energy barrier can be obtained.

However, if the solvent response is nonlinear, then the reactant free energy $G_{1a}(x,y)$ cannot be extrapolated by sampling about the free energy minimum and assuming a paraboloid shape. Instead, it will be vital to sample $G_{1a}(x,y)$ in regions far from its minimum where solvent response is nonlinear. Because we can relate G_{2b} to G_{1a} through eq 25, it follows that performing simulations on the VB state (2b) is equivalent to sampling G_{1a} with the additional biasing potential $x + y$, which allows us to probe regions that would otherwise remain sparsely sampled. This idea can be generalized by making use of the linearity of the solute−solvent charge interaction, which we assumed in eq 21. We first define variables η_{PT} and η_{ET} that represent the fraction of charge transferred from proton donor to acceptor and from electron donor to acceptor, respectively. Following ref 16 we can next define a fictitious partial charge transfer state (η_{PT},η_{ET}) (see Figure 3). By varying η_{PT} and η_{ET}, this state can take on the charge distributions of any of the four VB states (e.g., ($\eta_{PT} = 0,\eta_{ET} = 1$) corresponds to state (2a)). The assumption of linearity with respect to the solute−solvent interaction energy can be expressed as follows: if ϵ_η is the energy of the hypothetical partial charge transfer state (η_{PT},η_{ET}), then

$$\epsilon_\eta(\xi) = \Delta\epsilon_{PT}(\xi)\eta_{PT} + \Delta\epsilon_{ET}(\xi)\eta_{ET} + \epsilon_{1a}(\xi) \tag{65}$$

In analogy to eqs 23−25, we obtain the relation

$$G_\eta(x,y) = G_{1a}(x,y) + \eta_{PT}x + \eta_{ET}y + U_\eta - U_{1a} \tag{66}$$

where U_η is associated with the internal energy of the partial charge transfer state.

The introduction of the fictitious charge transfer state is the first element of our method to calculate accurate multidimensional free energy barriers. A similar technique has been used before in 1D systems.[16,19,25] By placing the solute in an arbitrary charge transfer state (η_{PT},η_{ET}), we can effectively move the location of the free energy minimum x_{1a} around which the solvent molecules fluctuate. This method is a type of importance sampling with a "biasing potential" of $x\eta_{PT} + y\eta_{ET}$ due to the partial charges on the donor/acceptor molecules. The biasing potential can be removed through eq 66. We can sample numerous charge transfer states to obtain a better global fit of the free energy surface. In fact, the common practice of sampling the reactant and product state can be seen as a special case of this more general scheme.

The second element of our method is our final nonquadratic fitting procedure. We will follow the method prescribed by Hummer et al.,[26] in which the cumulants of the simulation data are used to fit the numerical free energy to a multinomial form. If our sampling regions overlap sufficiently, we could attempt to reconstruct the free energy surface on a grid directly from the data without fitting it to some functional form. However, statistical error, especially far from the free energy minima, can be substantial. Additionally, we anticipate that the solvent response is locally linear, even if it is not globally linear. For this reason, we will use our simulation data to provide us only with the first- and second- derivatives of our free energy function evaluated at different values of x and y.

During a simulation of the partial charge transfer state (η_{PT},η_{ET}), the sample distribution of the variables $\Delta\epsilon_{PT}$ and $\Delta\epsilon_{ET}$ will be given by

$$P(\mathbf{x}) = N\exp(-\beta G_\eta(x,y)) \tag{67}$$

If the free energy function is locally quadratic about its minimum, then $P(\mathbf{x})$ will be Gaussian

$$P(\mathbf{x}) = N\exp(-\beta(\mathbf{x}-\mathbf{x}_\eta)A(\mathbf{x}-\mathbf{x}_\eta)) \tag{68}$$

where A is the Hessian matrix of $G_\eta(\mathbf{x})$ evaluated at is minimum $\mathbf{x}_\eta$. Then we can relate the expectation values $\langle\mathbf{x}\rangle$ and $\langle\mathbf{x}\mathbf{x}^T\rangle$ calculated from our simulation to the free energy parameters of $G_\eta(\mathbf{x})$

$$\mathbf{x}_\eta = \langle\mathbf{x}\rangle_\eta \tag{69}$$

$$\left.\frac{d^2G_\eta(\mathbf{x})}{d\mathbf{x}\,d\mathbf{x}^T}\right|_{\mathbf{x}=\langle\mathbf{x}\rangle_\eta} = \frac{1}{2\beta}(\langle\mathbf{x}\mathbf{x}^T\rangle_\eta)^{-1} \tag{70}$$

Furthermore, using eq 66, we can relate expectation values from our simulation to $G_{1a}(\mathbf{x})$

$$\left.\frac{dG_{1a}(\mathbf{x})}{d\mathbf{x}}\right|_{\mathbf{x}=\langle\mathbf{x}\rangle_\eta} = -\eta \tag{71}$$

$$\left.\frac{d^2G_{1a}(\mathbf{x})}{d\mathbf{x}\,d\mathbf{x}^T}\right|_{\mathbf{x}=\langle\mathbf{x}\rangle_\eta} = \frac{1}{2\beta}(\langle\mathbf{x}\mathbf{x}^T\rangle_\eta)^{-1} \tag{72}$$

These simulations provide us with local information about the first- and second-derivatives of $G_{1a}(\mathbf{x})$ evaluated at $\mathbf{x}_\eta$, which can be repeated for several values of η and used to globally fit $G_{1a}(\mathbf{x})$ to a multinomial.

Determining which charge transfer states to simulate can be accomplished in a number of ways. In general, it will certainly be necessary to sample the reactant state $\eta_{PT} = 0$,

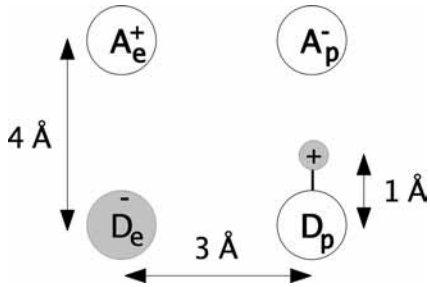

Figure 5. Schematic illustration of the configuration of donor and acceptor atoms used in the simulation. Static charges of +1 and −1 were placed on the electron acceptor and proton acceptor nuclei, respectively. Thus, in the reactant VB state (1a), the state shown in the figure, was a charged separated state. In contrast, the acceptor molecule in the product VB state (2b) is nearly nonpolar.

$\eta_{ET} = 0$. If the PCET process is in the normal region, then the transition state will probably lie close to the line joining the reactant and product states. Then a straightforward sampling scheme would sample linearly between the reactant $\eta_{PT} = 0$, $\eta_{ET} = 0$ and product $\eta_{PT} = 1$, $\eta_{ET} = 1$. However, we will see that in the Marcus inverted region, sampling techniques will need to be more subtle, since the transition state may lie far from the line joining the reactant and product wells. In Sec. IV, we sample the free energy surface on a 3 × 3 grid in the region between the product and reactant minima. In addition, we sample 5 additional locations to capture the inverted region of the free energy surface.

IV. Simulation Results

The model PCET system used in these simulations is shown in Figure 5. The D_e-D_p and A_e-A_p bond distances were held fixed at 3.0 Å. The D_p-A_p bond distance was held fixed at 4.0 Å, with the transferring proton located either 1.0 Å from the proton donor (in the reactant state, (1a)) or the proton acceptor (in the product state, (2b)). In the reactant state, the electron and proton are located on their donors, whereas in the product state, they are located on their acceptors. The electron and proton acceptors have permanent static charges of +1.0 and −1.0 respectively. The electron and proton have charges of −1.0 and +1.0, respectively, giving the solute complex an overall neutral charge. This model was chosen because it displayed significant nonlinear solvent response and could be used to test the adequacy of the linear response-based theories.

The solute was solvated in a cubic box of 240 TIP3P water molecules[27,28] with a side length of 19.0 Å. Solute−solvent and solvent-solvent interactions were modeled using electrostatic and van der Waals interactions. The van der Waals parameters for the interaction of the solute donors and acceptors with the oxygen of water were $\sigma = 3.5$ Å and $\epsilon = 0.15$ kcal/mol. Long range solvent-solvent electrostatic interactions were treated with an efficient Ewald approximation scheme.[29] A temperature of 300 K was maintained using a Nosé-Hoover thermostat[30,31] with a relaxation time of 0.4 ps as described in ref 32. Solvent dynamics were performed using the RATTLE algorithm[33] with a time step of 0.001 ps. The system was equilibrated for 100 ps, and data was collected for 15 ns.

In order to sample a large region of the free energy surface, simulations were performed using a range of partial charge transfer states (η_{PT},η_{ET}). The energy gap variables $\Delta\epsilon_{PT}$ and $\Delta\epsilon_{ET}$ were calculated every ten time steps (0.01 ps) throughout each simulation using eqs 18 and 19. Fourteen partial charge transfer states were used in all. The area of the free energy surface between the product and reactant minima was probed using a 3 × 3 grid of (η_{PT},η_{ET}) values, where η_{PT} and η_{ET} could each take on values of 0, 0.5, and 1.0. In the regions outside of this grid, the partial charge transfer states were (−0.5,0.5), (−0.5,0), (−0.5,−0.5), (0,−0.5), and (0.5,−0.5); these simulations probed the area on the free energy surface where the inverted region transition state is found. Using the method described in section III.C, the global free energy surface can be reconstructed from our numerical data. We used a sixth-order bivariate polynomial to fit $G_{1a}(\mathbf{x})$ to the simulation data according to eqs 71 and 72. $G_{2b}(\mathbf{x})$ can then be determined exactly from eq 25. Figure 6 shows the minimum free energy surface $\min\{G_{1a}(\mathbf{x}),G_{2b}(\mathbf{x})\}$ given an internal energy difference of $U_{2b} - U_{1a} = -100$ kcal/mol. In regions close to the minima, the two free energy surfaces are quadratic. However, at large displacements from equilibrium, clear deviations from linear solvent response are visible. Furthermore, the nonquadratic nature of the free energy surfaces causes the transition state to be displaced from the line connecting the two minima. Figure 7 shows that this effect is even more dramatic if we let $U_{2b} - U_{1a} = -270$ kcal/mol, which moves the reaction into the Marcus inverted region.

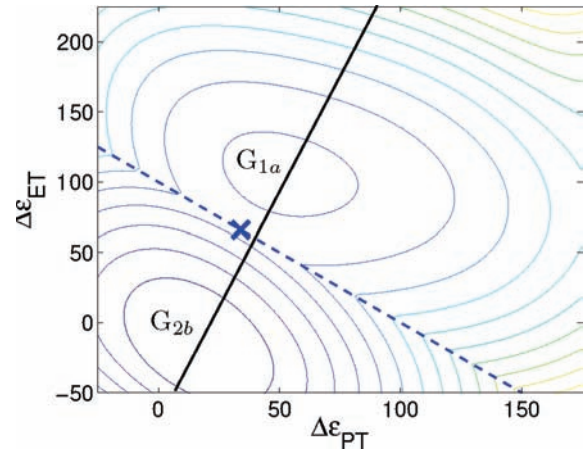

Figure 6. Minimum free energy surface $\min\{G_{1a}(\mathbf{x}),G_{2b}(\mathbf{x})\}$, assuming an internal energy difference of $U_{2b} - U_{1a} = -100$ kcal/mol; each contour represents approximately 8 kcal/mol. The intersection between the two surfaces is given by the dashed line, and the line connecting the two minima is shown in solid. The transition state is shown by the cross, and lies just away from the line connecting the minima, further indicating that the surface is nonquadratic.

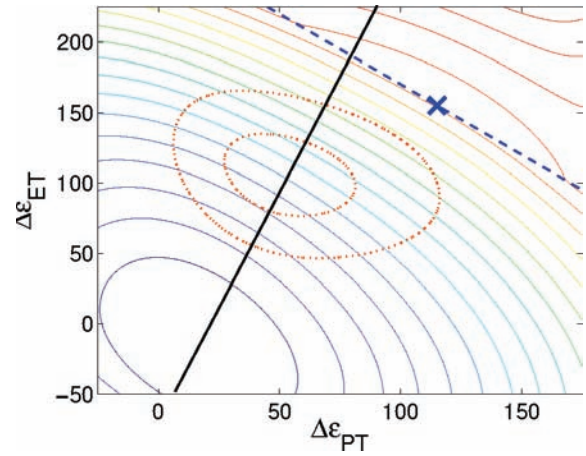

Figure 7. Same as Figure 6, assuming an internal energy difference of $U_{2b} - U_{1a} = -270$ kcal/mol; each contour represents approximately 14 kcal/mol. In this case, the reaction is in the Marcus inverted region, and the transition state lies far from the line connecting the minima, and thus the effects of nonquadraticity are quite pronounced.

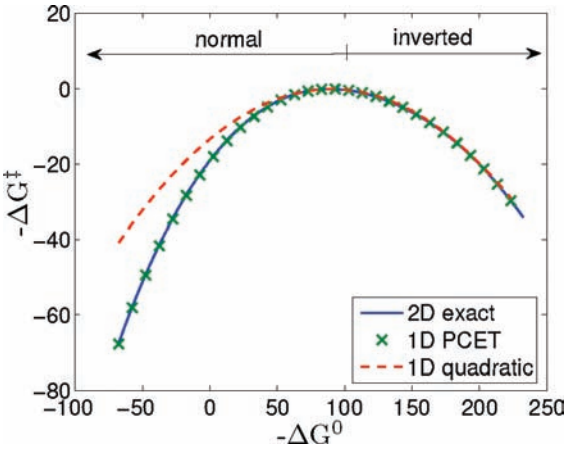

Figure 8. Evaluation of the effects of surface nonquadraticity on the calculation of 2D (solid) and reduced 1D PCET (crosses) activation energies. For a quadratic surface, the 2D and 1D barriers should agree exactly. In practice, near room temperature, even moderate surface nonquadraticity does not cause significant deviations of the 1D and 2D results. Also shown is the corresponding 1D activation energy resulting from a quadratic fit of the reduced 1D potential surface (dashed), highlighting the extent of the nonquadraticity.

Finally, we consider the effect of nonlinear solvent response on the reaction barrier $\Delta G^{\ddagger}$. In section III.B, it was shown that projecting the 2D free energy surface onto the reduced 1D PCET coordinate yields the exact 2D free energy barrier if the solvent response in linear. For a real, potentially nonlinear solvent, projecting onto the 1D PCET coordinate will yield a free energy barrier which deviates from the correct, 2D result. After projecting onto the 1D PCET coordinate, it is possible to make the further assumption that the free energy is a quadratic function of $\Delta\epsilon_{PCET}$, using the curvature of the free energy in the reactant well to extrapolate the free energy as in standard Marcus theory. Both the projection onto the PCET coordinate and the subsequent assumption of a quadratic free energy will yield free energy barriers that could potentially differ substantially from the exact, 2D result. Figure 8 shows the calculated free energy barrier as a function of ΔG^0 using both the real 2D free energy surface, the reduced 1D surface, and the 1D quadratic approximation. As expected, the 1D quadratic approximation is good in the inverted region, where the transition state is close to the reactant well. However, in the normal region, where the transition state is far from the reactant well, quadratic extrapolation gives poor results due to the nonlinearity of the solvent. We might have expected the same behavior for the 1D PCET approximation, but surprisingly, it gives very good results in both the normal and inverted region. In fact, while the agreement between 1D and 2D treatments is no longer perfect, the results are still nearly identical. Repeating the analysis at significantly higher temperature showed that the magnitude of these deviations increases with temperature. However near room temperature, any reasonable values for surface nonquadraticity led to only small deviations of the 1D approximation from the exact 2D results. This result is reassuring, since it implies that it may not be necessary to treat the PCET reaction in two dimensions, even if solvent response is nonlinear. On the other hand, the deviations of the 1D quadratic approximation in the normal regime highlight the well-known result that nonlinear solvent response necessitates sampling of multiple points on the 1D free energy surface.[26]

V. Conclusions

We have presented a general overview of multidimensional Marcus theory, highlighting many relevant theoretical results. In particular, we show that although a general description of multidimensional Marcus theory involves several independent solvation coordinates (in our case $\Delta\epsilon_{PT}$ and $\Delta\epsilon_{ET}$), the resulting reaction free energy barriers can be calculated equivalently from a 1D potential surface that is a function of a single collective solvent coordinate (in our case $\Delta\epsilon_{PCET} = \Delta\epsilon_{ET} + \Delta\epsilon_{PT}$). This reduces the computationally challenging calculation of 2D free energy surfaces to the straightforward task of 1D sampling. In the limit of quadratic surfaces, the resulting 2D and 1D reaction barriers are identical. We also demonstrated that, in the quadratic limit, the 2D reaction transition state always lies on the line connecting the reactant and product minima. Thus, the resulting 2D free energy reaction barriers can also be calculated by examining a slice through the 2D surface along this line segment, and the resulting 1D cross sections can be analyzed using conventional Marcus theory.

Finally, we examine the effects of surface nonquadraticity via molecular dynamics simulation for a particular model system of PCET. We reconstruct the full, 2D, nonquadratic surface based on several simulations with differing biasing potentials, and connect these results with a high-order fit. We find that, even for this moderately nonquadratic system near room temperature, the 2D and reduced 1D barrier description yield nearly identical results, although the location of the transition state is significantly more sensitive to the presence of surface nonquadraticity. However, since it is only the height, and not the location, of the reaction barrier that influences the reaction rate within the present theories, we thus conclude that the proposed method for barrier calculations based on the reduced 1D description is relatively robust with respect to nonlinear solvent effects. Our results help to justify the use of a single, 1D coordinate for the calculation of free energies barriers in multiple charge transfer systems.

Acknowledgment. The authors acknowledge support from National Science Foundation Grant No. CHE-0615882 and Department of Energy Grant No. DE-FG02-05ER15677.

References and Notes

(1) Marcus, R. A. *J. Chem. Phys.* **1956**, *24*, 966–978.
(2) Marcus, R. A. *Annu. Rev. Phys. Chem.* **1964**, *15*, 155–196.
(3) Marcus, R. A. *Rev. Mod. Phys.* **1993**, *65*, 599–610.
(4) Zusman, L. D.; Beratan, D. N. *J. Chem. Phys.* **1996**, *105*, 161.
(5) Soudackov, A.; Hammes-Schiffer, S. *J. Chem. Phys.* **1999**, *111*, 4672–4687.
(6) Hammes-Schiffer, S. *Acc. Chem. Res.* **2001**, *34*, 273–281.
(7) Soudackov, A.; Hammes-Schiffer, S. *J. Chem. Phys.* **2000**, *113*, 2385–2396.
(8) Marcus, R. *Angew. Chem., Int. Ed. Engl.* **1993**, *32*, 1111.
(9) Pérez, V.; Lluch, J. M.; Bertrán, J. *J. Am. Chem. Soc.* **1994**, *116*, 10117.
(10) Barbara, P. F. *J. Phys. Chem.* **1996**, *100*, 13148.
(11) Zusman, L. D. *Chem. Phys.* **1980**, *49*, 295.
(12) Warshel, A. *J. Phys. Chem.* **1982**, *86*, 2218–2224.
(13) We could equally choose $G_2(x)$ to be the "fundamental" free energy surface.
(14) Matyushov, D. M.; Voth, G. A. *J. Chem. Phys.* **2000**, *113*, 5413–5424.
(15) Small, D. W.; Matyushov, D. V.; Voth, G. A. *J. Am. Chem. Soc.* **2003**, *125*, 7478.
(16) Zhou, H.-X.; Szabo, A. *J. Chem. Phys.* **1995**, *103*, 3481–3494.
(17) Soudackov, A.; Hatcher, E.; Hammes-Schiffer, S. *J. Chem. Phys.* **2005**, *122*, 014505.
(18) Soudackov, A.; Hammes-Schiffer, S. *J. Am. Chem. Soc.* **1999**, *121*, 10598–10607.
(19) Hwang, J.-K.; Warshel, A. *J. Am. Chem. Soc.* **1987**, *109*, 715–720.

(20) Tachiya, M. *J. Phys. Chem.* **1993**, *97*, 5911–5916.
(21) Cukier, R. I.; Nocera, D. G. *Annu. Rev. Phys. Chem.* **1998**, *49*, 337–369.
(22) Hatcher, E.; Soudackov, A.; Hammes-Schiffer, S. *J. Phys. Chem. B* **2005**, *109*, 18565.
(23) Hatcher, E.; Soudackov, A.; Hammes-Schiffer, S. *J. Am. Chem. Soc.* **2007**, *129*, 187.
(24) Pechukas, P. *Annu. Rev. Phys. Chem.* **1981**, *32*, 159–177.
(25) King, G.; Warshel, A. *J. Chem. Phys.* **1990**, *93*, 8682–8692.
(26) Hummer, G.; Szabo, A. *J. Chem. Phys.* **1996**, *105*, 2004–2010.
(27) Jorgensen, W. L. *J. Am. Chem. Soc.* **1981**, *103*, 335.
(28) Jorgensen, W. L.; Chandrasekhar, J.; D., M. J.; Impey, R. W.; Klein, M. L. *J. Chem. Phys.* **1983**, *79*, 926.
(29) Adams, D. J.; Dubey, G. S. *J. Comp. Phys.* **1987**, *72*, 156–176.
(30) Nosé, S. *Mol. Phys.* **1984**, *52*, 255.
(31) Hoover, W. G. *Phys. Rev. A* **1985**, *31*, 1695.
(32) Häkkinen, H.; Manninen, M. *Phys. Rev. B* **1992**, *46*, 1725–1743.
(33) Andersen, H. C. *J. Comput. Phys.* **1983**, *52*, 24.

JP805065G